"Physics of Auroral Phenomena", Proc. XXXVI Annual Seminar, Apatity, pp. 130 - 132, 2013

Polar Geophysical Institute

ROLE OF TILT ORIENTATION OF BMRs AND MERIDIONAL CIRCULATION IN THE POLAR MAGNETIC FIELD REVERSAL ON THE SUN

N.V. Zolotova, D.I. Ponyavin (*St-Petersburg State University, St-Petersburg, Russia)*

Abstract. Using Greenwich catalogue of sunspots observations it was shown that impulses of sunspot activity during a course of solar cycle are responsible for residual magnetic field transported by meridional circulation toward the poles. This, in turn, is related to the polarity reversal of the axisymmetric large-scale magnetic fields. We perform parameter study of tilt angle of the Bipolar Magnetic Regions (BMRs) with imposed meridional flow profiles to model poleward magnetic field surges. Simulation was done in terms of point density distributions of leading and following sunspots according to Hale and Joy polarity rules. A faster meridional velocity reduces polar field. However results depend on size of the mesh grid. Latitudinal profile of meridional flow influences the polar field strength as well.

Introduction

The time-latitude diagram of the radial photospheric magnetic field of the Sun or the magnetic butterfly diagram (*Hathaway*, 2010) represents several main features: the 11-year periodicity of solar activity, Hale's law, Spörer's law, Joy's law, the reversal of the polar magnetic fields. Spots (or Bipolar Magnetic regions – BMRs) on the Sun emerge at latitudes of the so-called royal-zone. On time-latitude plane sunspots are distributed as impulses (*Antalová and Gnevyshev*, 1983). It was found that width of these impulses is some tens of degrees in latitude and duration from one 0.5 to 2 years. The times at which the impulses appear in both hemispheres commonly do not coincide. Also impulses may violate the Spörer's law, typically in long activity cycles (*Zolotova and Ponyavin*, 2012a).

The other "thin feature" of the magnetic butterfly diagram is intermittent polarity pattern of poleward streams from sunspot latitudes. These streams have been called magnetic surges by *Wang et al.* (1989), and explained as a result of meridional flow action on a diffusion background. *Wang et al.* (2002b) suggested that giant surges denote periods of increased flow velocity and amplified rate of flux emergence.

Currently to reproduce behavior of the polar magnetic fields the temporal changes of meridional flow velocity are popular to apply (*Schrijver and Liu*, 2008; *Wang et al.*, 2009; *Sheeley*, 2010; *Nandy et al.*, 2011). In the flux-transport model even a ~15% increase of flow velocity is enough to reproduce the 35–40% weaker polar field (*Wang et al*., 2009).

In this paper we reconstruct magnetic surges from sunspot impulses. To consider impact of only sunspot population to the surge strength we perform modeling without explicit diffusivity assignment. We consider influence of tilt angle of BMRs and latitudinal profile of the meridional flow on the strength and geometry of poleward surges.

Method

Fig. 1 schematically demonstrates procedure. Fig.1a displays modeled number of BMRs per day. The first cycle has symmetrical ascending and descending phases. The second one is long cycle; it reproduces the Waldmeier effect (*Waldmeier*, 1935). The third cycle is short double-peak cycle with the so-called Gnevyshev gap (*Gnevyshev*, 1963, 1967). Fig. 2b illustrates the butterfly diagram for these three cycles constructed as bivariate Gaussians. Parameters are described by *Zolotova and Ponyavin* (2012a). Each individual BMRs is shown according to the Joy's law. In asymmetrical case we define the latitudinal separation between leading and trailing spots of BMR as $\Delta l = \Delta d \cdot \tan(0.5 \cdot l)$, Δd is longitudinal separation, l is latitude. Fig. 1c illustrates probability density function (PDF) of BMRs:

$$f(X, \mu, \Sigma) = \frac{1}{\sqrt{|\Sigma|(2\pi)^d}} e^{\frac{1}{2}(X-\mu)\Sigma^{-1}(X-\mu)^T}$$

where $\boldsymbol{X} = (l, t)$ is 2-dimensional vector of sunspot positions on time-latitude plane with mean $\boldsymbol{\mu} = [\mu_l, \mu_t]$ and covariance matrix $\boldsymbol{\Sigma}$. $|\boldsymbol{\Sigma}|$ is determinant of the matrix $\boldsymbol{\Sigma}$ (Bishop, 2006). For convenience a flux in term of PDF is normalized according to its magnitude. Thus simulation is performed in dimensionless units. Now one can see that the first cycle was composed from one impulse in each hemisphere; the second — from two impulses; the third — from three impulses. In Fig. 1b overlapping of impulses hides internal structure of these cycles.

We set the magnetic flux from each sunspot impulse equal to its magnitude. Separate fluxes of leading and trailing spots: $Flux_{\text{trailing}}(l,t) = Flux_{\text{leading}}(l+\Delta l,t) \cdot 1.01$, where 1.01 is flux imbalance. In absence of diffusivity we specify a slight imbalance between leading and trailing fluxes of BMR – less than 10% for benefit of total flux of trailing spots in each hemisphere. Then we calculate flux surplus: $S(l,t) = Flux_{\text{leading}}(l,t) - Flux_{\text{trailing}}(l,t)$ (Fig. 1d). Finally, we use autoregression to reconstruct surges (Fig. 1e): $S_{\text{Result}}(l_{n+1}, t_{n+1}) =$

$S(l_{n+1},t_{n+1}) + S(l_{n+1} - \upsilon \cdot(t_{n+1} - t_n),t_n)$, where υ is velocity of meridional flow depending on latitude.

Fig. 1e illustrates that each activity impulse causes poleward surges. Actually, each impulse can generates both old and new polarity waves, but impulse geometry and their overlapping in time and latitude suppresses old polarity surges (*Zolotova and Ponyavin*, 2012a). Thereby, the poleward streams of old polarity are usually observed in gaps between impulses (see cycle composed of three impulses, Fig. 1e).

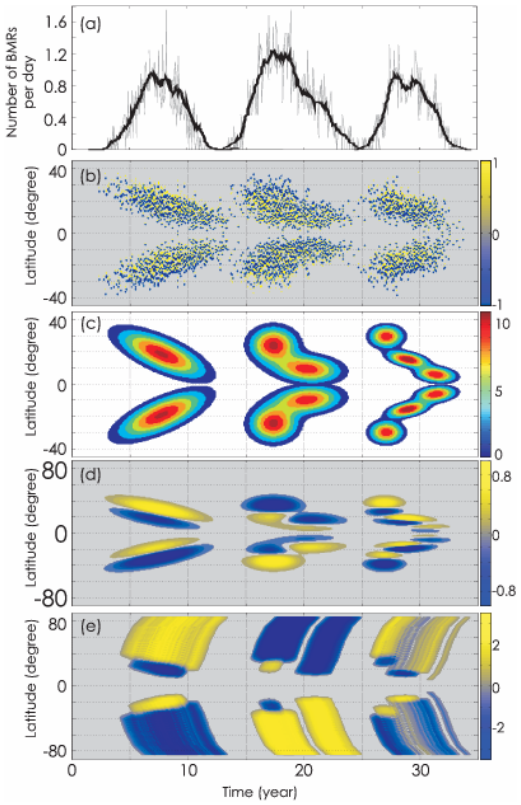

Fig. 1 (a) The cycle activity: number of BMRs per day — grey color, 6 months moving average — black color. **(b)** Modeled butterflies of individual BMRs. Yellow and blue define polarities. **(c)** Probability density function for BMRs. The color marks the levels of equal point density. **(d)** Surplus for modeled butterflies for Δd = 10° and υ_0 = 13 m s^{-1} at latitude 45°. **(e)** Reconstructed surges.

Parameter study

There are different approaches making use of latitude at which the meridional flow speed υ reaches a maximum:

-- 10°-20° (*DeVore & Sheeley*, 1987; *Wang et al.*, 2009; *Dikpati et al.*, 2010):

$$\upsilon(l) = \upsilon_0 \sin\left(\pi l / l_0\right),$$

where $\upsilon_0 = 13$ m s^{-1}, l_0 = 90°, see green dotted line on Fig. 2;

-- 35°-50° (*van Ballegooijen et al.*, 1998; *Schrijver & Title,* 2001; *Jiang et al.*, 2011b; *Hathaway & Rightmire*, 2011):

$$\upsilon(l) = \upsilon_0 \left(\sin l / \sin l_0\right)^p \left(\cos l / \cos l_0\right)^q,$$

where $\upsilon_0 = 13$ m s^{-1}, l_0 = 13.3°, p = 1, q = 0.1, see green dashed line on Fig. 2.

Additionally, to test we used two latitudinal profiles of latitudinal separation: Δd = 10° - orange solid line; Δd = 8° - orange thin line.

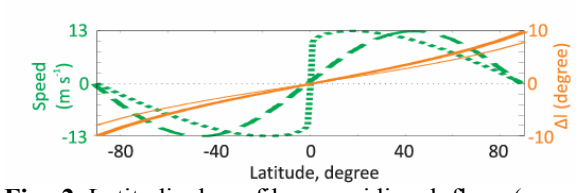

Fig. 2 Latitudinal profiles: meridional flow (green dotted and dashed), latitudinal separation Δl (orange solid and thin).

Fig. 3 illustrates parameters study for the RGO/USAF/NOAA daily data set from 1875 to 2012 (*Zolotova and Ponyavin*, 2013). Impulses are derived from sunspot positions (*http://solarscience.msfc.nasa.gov/greenwch.shtml*) by means of averaging of sunspot distribution on time-latitude plane (Fig. 3a). Colors denote equal levels of density. Parameters of sunspot impulses tracing are average window $dl \times dt$ = 0.6×1 and iteration step i = 20. Equal levels of density denote that populations of sunspot during the cycles 19, 21, and 22 are the highest.

Fig. 3b displays reconstructed magnetic poleward surges in dimensionless units $S_{\text{Result}}(l,t)$. In absence of background field and diffusion, each surge reaches polar latitudes. Flux surplus of leading polarity is evident at low latitudes, similarly to the real photospheric patterns (*Hathaway*, 2010).

Fig. 3c demonstrates smoothed over 10 Carrington rotations values of $S_{\text{Result}}(l,t)$ at latitudes 80° and −80°. Used parameters are Δd = 10° and υ_0 = 13 m s^{-1} at latitude 45°. Gleissberg cycle is evident (*Gleissberg*, 1967). Also from the Wilcox Solar Observatory (*http://wso.stanford.edu/*) it is known that magnitude of polar field decreases from cycle 21 to cycle 23. Similar regularity can be seen in Fig. 3c.

Fig. 3d illustrates the same values of $S_{\text{Result}}(l,t)$, but constructed for the following parameters: Δd = 10° and υ_0 = 13 m s^{-1} at latitude 13.3°. Magnitude of surges reaching the poles is reduced by almost half.

Fig. 3e shows the same values of $S_{\text{Result}}(l,t)$ for Δd = 8° and υ_0 = 13 m s^{-1} at latitude 45°. Magnitude of surges is slightly reduced. Finally, both an increase of the meridional flow speed toward the equator and vanished slope of tilt angle of BMRs against the latitude reduce strength of surges. However results depend on the size of mesh grid.

Wang et al. (2002a) observed that the strongest poleward surges occur near and just after sunspot maximum and are accompanied by fluctuations in the polar fields. Wang et al. (1989) suggested that such surges are generated by a combination of enhanced activity and large meridional flow speeds. We

suggest that strong surges are resulted primarily of enhanced activity (powerful sunspot impulses). Weak sunspot impulses and small tilt angle of BMRs at low latitudes reduce surges, which could not even reach the poles during the declining phase of solar cycles. We suggest that effect of the meridional flow is smaller in comparison influence of strength of sunspot impulses on magnitude of the polar field.

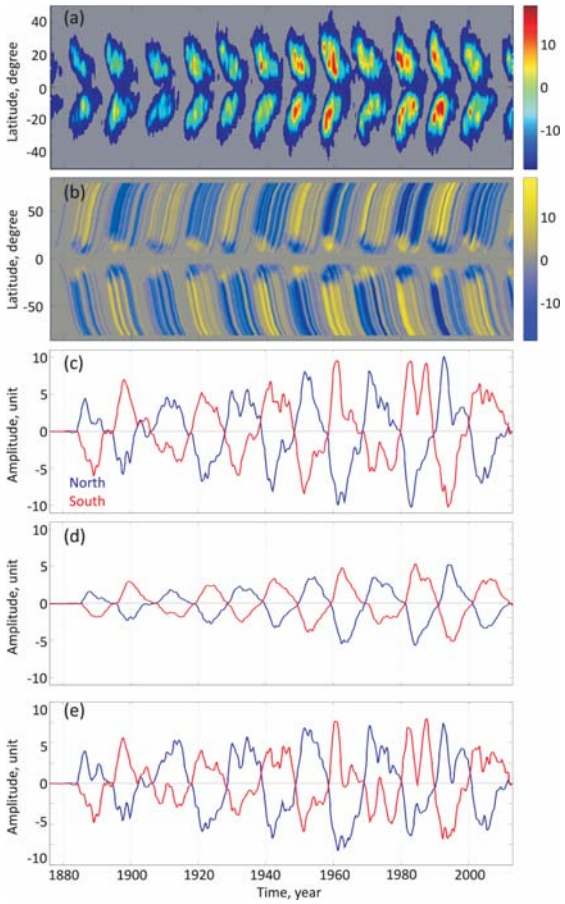

Fig. 3 (a) Sunspot impulses are constructed for average window $dl \times dt$ = 0.6×1 and iteration step i=20. **(b)** Reconstructed surges. **(c)** Smoothed northern and southern dimensionless values $S_{\text{Result}}(l,t)$ at latitudes 80° and −80°. Blue denotes the northern hemisphere and red – the southern hemisphere. Used parameters: Δd = 10° and v_0 = 13 m s^{-1} at latitude 45°. **(d)** The same for Δd = 10° and v_0 = 13 m s^{-1} at latitude 13.3°. **(e)** For Δd = 8° and v_0 = 13 m s^{-1} at latitude 45°.

Conclusions

In this paper, we performed parameter study of tilt angle (latitudinal segregation) of BMRs and meridional flow profile on poleward magnetic field surges. In our model polar large-scale magnetic fields are closely related to small-scale bipolar magnetic regions at low latitudes.

Variations in latitudinal profile of the meridional flow result in variations of simulated poleward surges. However further investigations are required due to dependence of findings on size mesh grid. The latitudinal profile of tilt angle of BMPRs also determines the strength of the polar field.

The polar field reversals are intimately related to the sunspot impulses. Their behavior exhibits long-term dynamical evolution. We suggest that weakening of the polar fields during the recent minimum is more associated with decrease in the field strength of sunspots (*Livingston and Penn*, 2009) and nominal sunspot counts (decrease of intensity of sunspot impulses) along the cycle 23 with respect to the cycles 21 and 22.

Acknowledgements. The work is supported by grant of the Russian Foundation for Basic Research 12-02-31108 mol_a.

References

Antalová, A., Gnevyshev, M. N., (1983). Contributions of the Astronomical Observatory Skalnate Pleso, 11, 63

Bishop, C. M. (2006). Pattern Recognition and Machine Learning, Springer, New York, 738

DeVore, C.R., Sheeley, N., Jr. (1987). Solar Phys., 108, 47

Dikpati, M., Gilman, P.A., Ulrich, R.K. (2010). Astrophys. J., 722, 774

Gleissberg, W. (1967). Solar Phys., 2, 231

Gnevyshev, M.N. (1963). Soviet Astronomy-AJ, 7, 3

Gnevyshev, M.N. (1967). Solar Phys., 1, 107

Hathaway, D.H. (2010). Living Reviews in Solar Physics 7, 1

Hathaway, D.H., Rightmire, L. (2011). Astrophys. J., 729, 80

Jiang, J., Cameron, R.H., Schmitt, D., Schüssler, M. (2011). Space Sci. Rev., 136

Livingston, W., Penn, M., (2009). EOSTr, 90, 257

Nandy, D., Mũnoz-Jaramillo, A., Martens, P. C. H. (2011). Nature, 471, 80

Schrijver, C. J., Liu, Y. (2008). Solar Phys., 252, 19

Schrijver, C.J., Title, A.M. (2001). Astrophys. J., 551, 1099

Sheeley, N. R., Jr. (2010), SOHO-23: Understanding a Peculiar Solar Minimum, 428, 3

van Ballegooijen, A.A., Cartledge, N.P., Priest, E. R. (1998). Astrophys. J., 501, 866

Waldmeier, M. (1935). Astron. Mitt. Eidgen. Sternw. Zürich, 14, 105

Wang, Y.-M., Lean, J., Sheeley, N.R., Jr. (2002a). Astrophys. J., 577, L53

Wang, Y.-M., Nash, A.G., Sheeley, N.R., Jr. (1989). Astrophys. J. 347, 529

Wang Y.-M., Robbrecht E., Sheeley N. R., Jr. (2009). Astrophys. J., 707, 1372

Wang, Y.-M., Sheeley, N.R., Jr., Lean, J. (2002b), Astrophys. J., 580, 1188

Zolotova, N.V., Ponyavin, D.I. (2008). IAUS 286: Comparative Magnetic Minima: Characterizing quiet times in the Sun and stars, 88

Zolotova, N.V., Ponyavin, D.I. (2012a). Astronomy Reports, 56, 250

Zolotova N.V., Ponyavin D.I. (2012b), Pulkovo annual solar physics conference Solar and Solar-Terrestrial physics – 2012, 47

Zolotova N.V., Ponyavin D.I. (2013), Geomagnetism and Aeronomy, in press.